

Molecular Biotechnology

Biochemical and mutational characterization of N-succinyl-amino acid racemase from *Bacillus stearothermophilus* CECT49

--Manuscript Draft--

Manuscript Number:	MOBI-D-14-00259R2
Full Title:	Biochemical and mutational characterization of N-succinyl-amino acid racemase from <i>Bacillus stearothermophilus</i> CECT49
Article Type:	Research Papers
Keywords:	N-succinyl-amino acid racemase; N-acyl-amino acid racemase; N-acetyl-amino acid racemase; racemase; acylase process; amino acid
Corresponding Author:	Sergio Martínez-Rodríguez, Ph.D. SPAIN
Corresponding Author Secondary Information:	
Corresponding Author's Institution:	
Corresponding Author's Secondary Institution:	
First Author:	Pablo Soriano-Maldonado
First Author Secondary Information:	
Order of Authors:	Pablo Soriano-Maldonado Montserrat Andújar-Sánchez Josefa María Clemente-Jiménez Felipe Rodríguez-Vico Francisco Javier Las Heras-Vázquez Sergio Martínez-Rodríguez, Ph.D.
Order of Authors Secondary Information:	
Abstract:	<p>N-succinyl-amino acid racemase (NSAAR), long referred to as N-acyl- or N-acetyl-amino acid racemase, is an enolase superfamily member whose biotechnological potential was discovered decades ago, due to its use in the industrial dynamic kinetic resolution methodology first known as "Acylase Process". In previous works, an extended and enhanced substrate spectrum of the NSAAR from <i>Geobacillus kaustophilus</i> CECT4264 toward different N-substituted amino acids was reported. In this work, we describe the cloning, purification and characterization of the NSAAR from <i>Geobacillus stearothermophilus</i> CECT49 (GstNSAAR). The enzyme has been extensively characterized, showing a higher preference toward N-formyl-amino acids than to N-acetyl-amino acids, thus confirming that the use of the former substrates is more appropriate for a biotechnological application of the enzyme. The enzyme showed an apparent thermal denaturation midpoint of 77.0 ± 0.1 °C and an apparent molecular mass of 184 ± 5 kDa, suggesting a tetrameric species. Optimal parameters for the enzyme activity were pH 8.0 and 55-65 °C, with Co²⁺ as the most effective cofactor. Mutagenesis and binding experiments confirmed K166, D191, E216, D241 and K265 as key residues in the activity of GstNSAAR, but not indispensable for substrate binding.</p>
Response to Reviewers:	As suggested, a grammatical/format revision of the manuscript has been carried out. These corrections have been marked in red in the text for easier localization.

Pablo Soriano-Maldonado^{a,b}, Montserrat Andújar-Sánchez^{a,b}, Josefa María Clemente-Jiménez^{a,b}, Felipe Rodríguez-Vico^{a,b}, Francisco Javier Las Heras-Vázquez^{a,b}, Sergio Martínez-Rodríguez^{a,b,*,#}.

^a *Dpto. Química y Física, Universidad de Almería, Campus de Excelencia Internacional Agroalimentario, ceiA3, 04120, Almería, Spain.*

^b *Centro de Investigación en Biotecnología Agroalimentaria, BITAL. Almería, Spain.*

* **Corresponding author:** Sergio Martínez-Rodríguez

Dpto. Química y Física.

Universidad de Almería.

Edificio CITE I, Carretera de Sacramento s/n.

04120 La Cañada de San Urbano, Almería (Spain)

srodrig@ual.es

[#]Actual address, Department of Physical Chemistry, University of Granada, 18071, Granada, Spain. sergio@ugr.es

Acknowledgements

We thank Andy Taylor for critical discussion of the manuscript and Pedro Madrid-Romero for technical assistance.

Funding

This work was supported by the Spanish Ministry of Education and Science, the European Social Fund (ESF), and the European Regional Development Fund (ERDF), through the project BIO2011-27842, by the Andalusian Regional Council of Innovation, Science and Technology, through the project TEP-4691, and by the European Cooperation in Science and Technology (COST) Action CM1303. P.S.-M. was supported by the University of Almería. S.M.-R. was supported by the Spanish Ministry of Science and Innovation.

1 **Biochemical and mutational characterization of *N*-succinyl-amino acid**
2 **racemase from *Geobacillus stearothermophilus* CECT49**

3

4 **Keywords:** *N*-succinyl-amino acid racemase, *N*-acyl-amino acid racemase, *N*-acetyl-
5 amino acid racemase, acylase process, amino acid.

6

7 **Abstract**

8 *N*-succinyl-amino acid racemase (NSAAR), long referred to as *N*-acyl- or *N*-acetyl-
9 amino acid racemase, is an enolase superfamily member whose biotechnological
10 potential was discovered decades ago, due to its use in the industrial dynamic kinetic
11 resolution methodology first known as “Acylase Process”. In previous works, an
12 extended and enhanced substrate spectrum of the NSAAR from *Geobacillus*
13 *kaustophilus* CECT4264 toward different *N*-substituted amino acids was reported. In
14 this work, we describe the cloning, purification and characterization of the NSAAR
15 from *Geobacillus stearothermophilus* CECT49 (GstNSAAR). The enzyme has been
16 extensively characterized, showing a higher preference toward *N*-formyl-amino acids
17 than to *N*-acetyl-amino acids, thus confirming that the use of the former substrates is
18 more appropriate for a biotechnological application of the enzyme. The enzyme showed
19 an apparent thermal denaturation midpoint of 77.0±0.1 °C and an apparent molecular
20 mass of 184±5 kDa, suggesting a tetrameric species. Optimal parameters for the enzyme
21 activity were pH 8.0 and 55-65 °C, with Co²⁺ as the most effective cofactor.
22 Mutagenesis and binding experiments confirmed K166, D191, E216, D241 and K265 as
23 key residues in the activity of GstNSAAR, but not indispensable for substrate binding.

24

25

26 **Introduction**

27 *N*-succinyl-amino acid racemase (NSAAR), long referred to as *N*-acyl- or *N*-acetyl-
28 amino acid racemase (NAAR)¹, is an enolase superfamily member whose
29 biotechnological potential was discovered decades ago, due to its use in the industrial
30 dynamic kinetic resolution (DKR) methodology first known as “Acylase Process” [1].
31 Though this enzyme has been mainly studied because of its *N*-acetyl-amino acid
32 racemase activity [1-9], its catalytic promiscuity attracted the attention of several
33 scientists, whose work on the evolution and real classification of these enzymes [10-16]
34 led them to propose its classification as a NSAAR [16,17]. This enzyme belongs to the
35 mechanistically diverse enolase superfamily, and in fact, it is an example of real
36 catalytic promiscuity, since it is active toward many different substrates [10].

37

38 Despite a high number of patents describing the use of NSAAR/NAAR [18-24], and
39 works related to the isolation of microorganisms showing this activity [2, 25], only a
40 small number of NSAAR/NAAR enzymes have been described in detail in the
41 literature. In fact, only the enzymes belonging to *Amycolatopsis* [1,2,3,6,7,26],
42 *Deinococcus* [8,27-30], *Streptomyces* [3] and *Geobacillus* [9,16,31-33] have been
43 characterized to different extents. The crystallographic structure of *Thermus*
44 *thermophilus* HB8 NAAAR has also been reported, but its activity has not been
45 described [34]. Besides *N*-acetyl-amino acids, NSAAR/NAAR enzymes have also been
46 reported to racemize other *N*-substituted amino acids to very different extents
47 [3,4,6,7,9,16,32,33,35]. The recombinant NSAAR from *Geobacillus kaustophilus*
48 CECT4264 (GkaNSAAR) proved to racemize *N*-formyl-amino acids more efficiently
49 than the industrially used acyl- derivatives [31], allowing us to develop a more general

¹We will use the three names indistinctly during this work, to try to maintain the original nomenclature used in the corresponding papers.

50 and efficient DKR method based on the “Acylase Process” (namely Amidohydrolase
51 Process) by coupling it with a stereospecific L-N-carbamoylase (Figure 1) [32,33].
52 Motivated by the potential of NSAAR enzymes in DKR processes for optically pure D-
53 and L-amino acid production [28-30,36], a recent paper highlights the efforts carried out
54 to engineer improved NSAAR enzymes for this purpose [35]. Accordingly, it seems
55 clear that finding new enzymes with improved characteristics or broader substrate
56 spectrum would enhance this DKR methodology, since NSAAR enzymes constitute the
57 limiting step for reaction in the bienzymatic tandems where this enzyme has been
58 applied [28-30,32,33,35].

59

60 In this work, we have cloned, overexpressed, purified and characterized the NSAAR
61 belonging to *Geobacillus stearothermophilus* CECT49 (GstNSAAR), specifically
62 evaluating its N-formyl-amino acid racemase activity, since this activity has not been
63 previously studied in detail for any NSAAR enzyme. In order to provide additional
64 information on the mechanism and enzymatic features of NSAAR enzymes, we
65 specifically altered five amino acids in the catalytic center of the enzyme to investigate
66 their biochemical role in binding and catalysis.

67

68 **Material and Methods**

69 *Materials*

70 All chemicals were of analytical grade and were used without further purification.
71 Restriction enzymes and T4 DNA ligase were purchased from Roche Diagnostic S.L.
72 (Barcelona, Spain). Kapa-Hifi polymerase was from Cultek S.L.U. (Madrid, Spain).
73 Primers were from IDT (Biomol, Spain). TALONTM metal affinity resin was purchased
74 from Clontech Laboratories, Inc. Racemic and optically pure amino acids and N-acetyl-

75 methionine were from Sigma Aldrich Quimica S.A. (Madrid, Spain). The *N*-carbamoyl-
76 , *N*-succinyl- and *N*-formyl-amino acids were synthesized according to previous works
77 [9, 32-33].

78

79 *Microbes and culture conditions*

80 *Geobacillus stearothermophilus* CECT49 and *Deinococcus radiodurans* CECT833
81 were used as possible donors of different *N*-succinyl-amino acid racemase (*nsaar*)
82 genes. *Geobacillus stearothermophilus* CECT49 was grown on nutrient broth/agar I
83 plates (1% peptone, 0.5% beef extract, 0.5% NaCl, pH 7.2, 1.5% Agar) at 55 °C (24 h).
84 *Deinococcus radiodurans* CECT833 was grown on *Corynebacterium* broth/agar plates
85 (1% casein peptone (tryptic digest); 0.5% yeast extract, 0.5% glucose, 0.5% NaCl, 1.5%
86 Agar) at 30 °C (72 h). *Escherichia coli* DH5α was used to clone the different putative
87 *nsaar* genes, and *E. coli* BL21 (DE3) to overexpress the proteins.

88

89 *Cloning of N-succinyl-amino acid racemase (nsaar) genes*

90 A single-colony isolate of *Geobacillus stearothermophilus* CECT49 and *Deinococcus*
91 *radiodurans* CECT833 strains was chosen for DNA extraction by a boiling procedure.
92 A sample of the supernatant containing genomic DNA (5 µl) was used to amplify the
93 different **fragments** encoding for putative *nsaar* genes by PCR. Each of the obtained
94 PCR fragments was purified from agarose gels using QIAquick (Qiagen) and then
95 subcloned using a StrataClone™ PCR Cloning Kit (Stratagene). The isolated sub-
96 cloning plasmids were purified using QIAprep Spin miniprep kit (Qiagen), and digested
97 using *NdeI/XhoI* (*Deinococcus radiodurans* CECT833 gene, *drcnsaar*) or *SacI/BamHI*
98 (*Geobacillus stearothermophilus* CECT49 gene, *gstnsaar*). The digested fragments
99 were purified from agarose gel using QIAquick (Qiagen), and then the *drcnsaar* gene

100 was ligated into *NdeI/XhoI* site of pET22b+ plasmid (Novagen), and *gstnsaar* gene into
101 the *SacI/BamHI* site of the rhamnose-inducible expression vector pJOE4036.1 [37]. The
102 resulting constructions allowed the production of the *Geobacillus stearothermophilus*
103 CECT49 NSAAR (GstNSAAR) and *Deinococcus radiodurans* CECT833 (DrcNSAAR)
104 enzymes with a C-terminal His₆-tag. The cloned DNA fragments were sequenced using
105 the dye dideoxy nucleotide sequencing method in an ABI 377 DNA Sequencer (Applied
106 Biosystems). Translated sequences were aligned and compared with other available
107 amino acid sequences using the Basic Local Alignment Search Tool (BLAST, NCBI).
108 Clustal W-XXL was used for alignment [38].

109

110 *Expression of GstNSAAR and DrcNSAAR*

111 The different plasmids were transformed into *E. coli* BL21 (DE3) and then grown in LB
112 medium supplemented with 100 µg·ml⁻¹ of ampicillin. A single colony was transferred
113 into 10 ml of LB medium supplemented with 100 µg·ml⁻¹ of ampicillin in a 100 ml
114 flask, and these cultures were incubated overnight at 37 °C with shaking. 500 ml of LB
115 supplemented with 100 µg·ml⁻¹ of ampicillin were inoculated with 5 ml of the overnight
116 culture in a 2 l flask. After 2 h of incubation at 37 °C with vigorous shaking, the OD₆₀₀
117 of the resulting cultures was 0.3-0.5. For expression induction of the putative *gstnsaar*
118 and *drcnsaar* genes, L-rhamnose (0.2%) or isopropyl-β-thio-D-galactopyranoside
119 (IPTG, 0.2 mM) were added to the cultures, respectively. The cultures were continued
120 for a further 6 hours at 32 °C and 34 °C, respectively. The cells were collected by
121 centrifugation (Beckman JA2-21, 7,000 g, 4 °C, 20 min), and stored at -20 °C until use.
122 Overexpression of GkaNSAAR enzyme was carried out as previously described [32].

123

124

125 *Purification of GstNSAAR, DrcNSAAR and GkaNSAAR enzymes*

126 Recombinant *E. coli* cells were resuspended in 30 ml wash buffer (300 mM NaCl,
127 0.02% NaN₃, 50 mM sodium phosphate pH 7.0). The cell walls were disrupted in ice by
128 sonication using a UP 200 S Ultrasonic Processor (Dr. Hielscher GmbH) for 6 periods
129 of 30 s, pulse mode 0.5 and sonic power 60%. The pellet was precipitated by
130 centrifugation (Beckman JA2-21, 10,000 g, 4 °C, 20 min) and discarded. The
131 supernatant was applied to a column packed with cobalt metal affinity resin and then
132 washed three times with wash buffer (see above). NSAAR enzymes were eluted with
133 elution buffer (100 mM NaCl, 0.02% NaN₃, 50 mM imidazole, 2 mM Tris, pH 8.0).
134 Protein purity was determined at different stages of the purification by SDS-PAGE
135 electrophoresis. An additional gel filtration chromatography step was carried out using a
136 Superdex 200 gel filtration column (GE Healthcare) in a BioLogic DuoFlow FPLC
137 system (BioRad) to eliminate any DNA co-eluting with the protein, with observation at
138 280 nm. The purified enzyme was concentrated using an Amicon ultrafiltration system
139 with Amicon YM-3 membranes, dialyzed against 100 mM Borate-HCl pH 8.0 and
140 stored at 4 °C. Protein concentrations were determined from the absorbance of
141 coefficient extinction of tyrosine residues [39].

142

143 *Standard Enzymatic assay*

144 A standard enzymatic reaction was carried out to assess the activity of GstNSAAR,
145 DrcNSAAR and GkaNSAAR enzymes toward different *N*-substituted-amino acids.
146 Purified enzymes (0.1-50 μM) were incubated together with different *N*-substituted-
147 amino acids (15 mM), using 100 mM Borate/HCl buffer 1.6 mM CoCl₂ pH 8.0 (500 μl
148 reaction volume). The reaction mixture was incubated at 45 °C, and aliquots of 75 μl
149 were retrieved at different times and boiled at 95 °C for 5 min to stop the enzymatic

150 reaction. Then, 675 μ l of the corresponding mobile phase (see below) was added to the
151 stopped sample before centrifugation (13,000 rpm, 10 min). Samples were analyzed in a
152 HPLC system (LC2000Plus HPLC System, Jasco) equipped with a Chirobiotic T
153 column (4.6 mm x 250 mm, ASTEC Inc., USA). The mobile phase was 70% methanol,
154 30% ammonium acetate (0.01 M), and 0.5 ml acetic acid per liter [33], pumped at a
155 flow rate of 0.6 ml·min⁻¹ and measured at 200 nm. The specific activity of the enzymes
156 was defined as the amount of enzyme that catalyzed the formation of 1 mmol of *N*-D- or
157 *N*-L-substituted amino acid per min and mg of protein at 45 °C.

158

159 *Characterization of GstNSAAR enzyme*

160 In order to get the apo-form of GstNSAAR, freshly purified enzyme (2.3 μ M) was
161 incubated overnight with 25 mM HQSA, followed by extensive dialysis in 100 mM
162 Borate-HCl buffer pH 8.0. To analyze the effect of different cations on GstNSAAR
163 activity, apo-GstNSAAR was incubated separately in the presence of 2 mM NaCl, KCl,
164 LiCl, CsCl, RbCl, MgCl₂, CaCl₂, ZnCl₂, CoCl₂, NiCl₂, FeCl₂, PbCl₂, HgCl₂ in 100 mM
165 Borate-HCl buffer pH 8.0 (final volume 20 μ l) at 4 °C for 60 minutes, followed by the
166 standard enzyme assay. The standard enzyme assay was used to determine optimum
167 temperature and pH of GstNSAAR. The temperature range was 20 to 85 °C and the
168 buffers used were 100 mM sodium citrate (pH 4.0-6.0), 100 mM sodium phosphate (pH
169 6.0-8.0), 100 mM sodium Borate-HCl (pH 8.0-9.0), Tris-HCl (pH 7.5-9.0) and 100 mM
170 Borate-NaOH (pH 9.0-10.5). Thermal stability of the enzyme (2.3 μ M) in 100 mM
171 Borate-HCl buffer pH 8.0 was determined after 60-min preincubation at different
172 temperatures from 20 to 85 °C in the absence or presence (1.6 mM) of CoCl₂, followed
173 by the standard activity assay. Kinetic studies of GstNSAAR were conducted using
174 different *N*-formyl-D- and *N*-formyl-L-amino acids as substrate in 100 mM Borate-HCl

175 buffer 1.6 mM CoCl₂ pH 8.0 following the standard assay, with concentrations of
176 substrate up to 50 mM. The activity of GstNSAAR mutants was measured using the
177 standard activity assay described above, increasing enzyme concentration up to 50 μM.

178

179 *Alanine scanning of GstNSAAR K166, D191, E216, D241 and K265*

180 Mutagenesis was performed using QuikChange II Site-directed mutagenesis kit from
181 Stratagene following the manufacturer's protocol, using the pET22b+ plasmid
182 containing GstNSAAR as template. Mutations were confirmed by using the dye
183 dideoxy nucleotide sequencing method in an ABI 377 DNA Sequencer (Applied
184 Biosystems). The plasmids containing the mutated residues (K166A, D191A, E216A,
185 D241A, K265A), were transformed into *E. coli* BL21 (DE3) and protein overexpression
186 and purification were carried out as described above for the wild-type enzyme.

187

188 *Circular Dichroism experiments*

189 The secondary structures of GstNSAAR mutants (K166A, D191A, E216A, D241A and
190 K265A) were compared to the wild-type GstNSAAR using far-UV circular dichroism
191 (CD) spectra, recorded with a Jasco J850 CD spectrometer (Jasco Inc.) equipped with a
192 JASCO PTC-423S/15 Peltier accessory. Experiments were acquired with a response
193 time of 8 s, a bandwidth of 1 and a step resolution of 0.2 nm. Protein concentrations
194 were 2-6 μM in 10 mM Borate-HCl buffer pH 8.0. CD measurements were taken at 25
195 °C using a 1-mm path-length cuvette. Spectra were acquired from 250 to 190 nm at a
196 scan rate of 50 nm·min⁻¹, and averaged over 5 scans.

197

198 For thermal denaturation experiments, CD spectra were measured in 100 mM Borate-
199 HCl buffer 1.6 mM CoCl₂ pH 8.0 at a protein concentration of 5 μM in a 0.1 mm

200 cuvette. Thermal denaturation measurements were monitored by measuring the changes
201 in ellipticity at 222 nm. Denaturation data were collected at a scan rate of 0.2 °C·min⁻¹
202 and the temperature was increased from 25 to 95 °C.

203

204 *Binding experiments with GstNSAAR mutants*

205 Fluorescence emission spectra were measured at 25 °C using an FP-6500
206 spectrofluorimeter (Jasco Inc.) equipped with an ETC 273T Peltier accessory with the
207 proper excitation and emission wavelengths, using a cell of 1 cm path length. Enzymes
208 were excited at 280 nm in order to obtain the intrinsic fluorescence spectra. The binding
209 of *N*-formyl-D- or *N*-formyl-L-methionine to alanine mutants of GstNSAAR was
210 monitored using the decrease in fluorescence emission at 341 nm. Excitation and
211 emission bandwidths were 3 nm. Fluorescence measurements were corrected for
212 dilution.

213 The saturation fraction, *Y*, can be expressed as:

$$214 \quad Y = \frac{K[\text{Ligand}]}{1 + K[\text{Ligand}]} \quad (1)$$

215 where *K* is the characteristic microscopic association constant and [*Ligand*] is the free
216 concentration of *N*-formyl-D- or *N*-formyl-L-methionine. The saturation fraction, *Y*, can
217 be calculated as:

$$218 \quad Y = \frac{\Delta F_{\text{corr}}}{\Delta F_{\text{corr}}^{\text{max}}} = \frac{F(\text{Ligand}) - F(0)}{F(\infty) - F(0)} \quad (2)$$

219 where *F*(0), *F*(*Ligand*) and *F*(∞) are the corrected fluorescence intensities for the protein
220 solution without ligand, at a concentration of ligand equal to *N*-formyl-D- or *N*-formyl-
221 L-methionine and at saturating ligand concentration, respectively.

222

223

224 **Results and Discussion**

225 *Sequence analysis of GstNSAAR and DrcNSAAR*

226 A BLASTn search with the nucleotide sequence of *Geobacillus stearothermophilus*
227 CECT49 revealed 99% identity with the locus tag GK0926 from *Geobacillus*
228 *kaustophilus* HTA426 (GenBank acc. No BA000043, region 949470-950594; prot
229 BAD75211.1) and 97% identity with the previously isolated *N*-succinyl-amino acid
230 racemase gene from *Geobacillus kaustophilus* CECT4264 (EU427322.1). On the other
231 hand, the BLASTn search with the nucleotide sequence of *Deinococcus radiodurans*
232 CECT833 NSAAR genes revealed 100% identity with the locus tag DR_0044 from
233 *Deinococcus radiodurans* R1 (GenBank acc. No AE000513, region 42775-43899; prot
234 AAF09631.1). The translated sequences of both genes were used to carry out a
235 sequence alignment with the other NSAAR enzymes described in the literature for
236 which the sequence is available (Figure 2). As expected, the higher sequence identities
237 of GstNSAAR and DrcNSAAR were found with those of the other NSAAR from the
238 same genera (GstNSAAR and GkaNSAAR, 97.6% seq. id.; DrcNSAAR and
239 *Deinococcus radiodurans* CCRC 12827 (DraNSAAR, [8]); 98.7% seq. id.)). Similar
240 results were obtained with other NSAAR from the same genera (*Amycolatopsis*
241 *orientalis* subsp. *lurida* and *Amycolatopsis azurea*; 95.1% seq. id.). The *Geobacillus*
242 and *Deinococcus* NSAARs shared a 47-48% of seq. id. Sequence identities of
243 GstNSAAR and DrcNSAAR with the other NSAAR from *Amycolatopsis* and *Thermus*
244 were 42.8-48.5% and 43.6-59.7%, respectively. A recent work already highlighted that
245 NSAARs cannot be easily segregated into a family separate from the OSBS family, due
246 to the high levels of sequence similarity and the bifunctionality shown by several of
247 some OSBS/NSAAR family enzymes [40]. This fact would clearly explain why only
248 the activity of NSAARs from five different microbial genera (see above) has been

249 described in the literature (decreasing to three cases for which sequence-activity
250 relationship has been proved; *Geobacillus*, *Deinococcus* and *Amycolaptosis*). Eight
251 subfamilies into the OSBS family of enzymes have been differentiated [40]; one of
252 them is the so-called *Firmicutes* OSBS/NSAAR subfamily, where the enzymes with
253 proven NSAAR activity (*Geobacillus*, *Deinococcus* and *Amycolaptosis*) and that from
254 *Thermus* are included. However, this subfamily also contains OSBS enzymes without
255 NSAAR activity, such as *Bacillus subtilis* YtfD, sharing more than 40% of sequence
256 identity with NSAAR of proven activity [10]. Thus, a BLAST search strategy intended
257 to look for new real NSAAR enzymes with potential biotechnological application might
258 not be the most successful strategy, even if a high sequence identity cut-off is used,
259 since as denoted above, sequences showing 40-50% sequence identity do not always
260 encode enzymes with NSAAR activity.

261

262 *Expression and purification of NSAAR enzymes*

263 Purification of GstNSAAR and DrcNSAAR enzymes yielded 5-20 mg of protein *per*
264 liter of the recombinant *E. coli* culture. SDS-PAGE analysis indicated that the different
265 enzymes were over 95% pure after elution of the affinity column (Figure 3), with an
266 estimated molecular mass of 43 kDa (the deduced mass from the amino acid sequences,
267 including the His₆-tag, is in the 43-44 kDa range). SEC-experiments conducted on a
268 Superdex 200 10/300 column showed that GstNSAAR eluted at 15.2 mL (Figure 3),
269 corresponding to an apparent molecular mass of 184±5 kDa. Since the theoretical
270 molecular mass of a GstNSAAR tetramer is 174.3 kDa, our results suggests a tetrameric
271 species (or a compacted higher-order oligomer). Similar results were obtained
272 previously with GkaNSAAR (170-177 kDa) [31]. The NSAAR from *Streptomyces*
273 *atratus* Y-53 (SatNSAAR) was described as an hexamer [3], whereas the enzymes

274 belonging to *Amycolaptosis* [4,6,7] and *Deinococcus* [8] genera have been reported as
275 octamers.

276

277 *Characterization of GstNSAAR enzyme*

278 Activity of GstNSAAR was assayed in the presence of different metal cations (Table 1).

279 All the tested cations increased the activity of the apoenzyme, although cobalt exerted

280 the highest increase. GstNSAAR enzyme was also active after IMAC purification

281 (43.2±0.4% relative activity compared to the Co-amended enzyme), most likely due to

282 the NaCl present in the elution buffer, or even to Co²⁺ leakage from the IMAC column

283 used for purification. Similar results have been shown with other NSAAR enzymes [3-

284 9], although Mg²⁺ has been reported as the normal divalent metal ion utilized by

285 members of the enolase superfamily [41]. Thus, all the characterization of GstNSAAR

286 was carried out in the presence of this cofactor. GstNSAAR showed maximum activity

287 at pH 8.0-8.5 and 55-65 °C. Similar results have been shown for other NSAAR enzymes

288 ranging pHs 7.5-8.0 and 40-60 °C [3-9]. Thermal stability of GstNSAAR was studied by

289 means of two techniques: 1) pre-incubating the enzyme in 100 mM Borate-HCl buffer

290 pH 8.0 at different temperatures for 60 min, and subsequently measuring the residual

291 activity; and 2) following the denaturation melting curve by means of far-UV CD.

292 Activity was gradually lost when the enzyme was incubated in the absence of Co²⁺ at

293 temperatures over 45 °C, and over 55 °C when Co²⁺ was present during the

294 preincubation (Figure 4). Similar results have been observed previously for

295 GkaNSAAR, showing that the presence of the cation in the protein produces a

296 stabilization of approximately 10 °C [31]. In view of this decrease in activity over 55 °C,

297 we decided to carry out all subsequent reactions at 45 °C.

298

299 Although the thermal denaturation followed by far-UV CD (Figure 4) was irreversible,
300 and therefore it was not possible to estimate the thermodynamic parameters governing
301 thermal unfolding (ΔH_{vH}), we determined an apparent thermal denaturation midpoint
302 ($T_{m(app)}$), as has been described for other proteins showing irreversible thermal
303 denaturations [42,43]. The $T_{m(app)}$ for GstNSAAR was 77.0 ± 0.1 °C (Table 3),
304 confirming an apparent moderate thermostability of GstNSAAR, similar to that
305 previously obtained with other NSAAR enzymes [9,31]. The differences shown
306 between the $T_{m(app)}$ and the midpoint calculated from the residual activity after
307 preincubation (Figure 4; approximately 15 °C) can be explained by the Equilibrium
308 Model [44,45]: enzymatic activity might be lowered or lost below the apparent
309 unfolding temperature as a result of temperature-induced conformational changes at the
310 active site from an optimum configuration for substrate binding to a less optimum one.
311 Previous results with GkaNSAAR showing a different optimal temperature for *N*-
312 formyl- and *N*-carbamoyl-amino acid racemization [32] also support temperature-
313 induced conformational changes of the catalytic center.

314

315 *Substrate specificity of GstNSAAR*

316 Whereas the major efforts on the activity characterization of NSAAR/NAAR enzymes
317 have been focused on their *N*-acetyl-racemase activity, NSAAR/NAAR enzymes
318 belonging to *Streptomyces*, *Amycolatopsis*, *Deinococcus* and *Geobacillus* have also
319 been reported to racemize to very different extents other *N*-substituted-amino acids such
320 as *N*-propionyl-, *N*-butyryl-, *N*-benzoyl-, *N*-acetyl-, *N*-chloroacetyl-, *N*-carbamoyl-, *N*-
321 succinyl- and *N*-formyl-amino acids [3,4,6,7,9,16,32,33,35]. *Streptomyces* and
322 *Amycolatopsis* NAARs are able to racemize *N*-formyl-amino acids (more slowly than
323 the acylated species) [3,4], but GkaNSAAR was the first NSAAR enzyme reported to

324 racemize *N*-formyl-amino acids much faster than *N*-acetyl- or *N*-carbamoyl-amino acids
325 [9]. In order to compare the catalytic properties of GstNSAAR and DrcNSAAR
326 enzymes with those of previously characterized NSAAR enzymes, we also purified
327 GkaNSAAR enzyme [9]. The enzymes were firstly confirmed to be active towards *N*-
328 succinyl-D- and L-phenylalanine (Table 2). GstNSAAR and DrcNSAAR were also
329 active to different degrees toward *N*-acetyl-, *N*-carbamoyl- and *N*-formyl-amino acids
330 (Table 2). Under the reaction conditions, GstNSAAR and GkaNSAAR were more
331 efficient in all cases than DrcNSAAR (Table 2). Interestingly, although DraNSAAR has
332 been mainly characterized and used for its *N*-acetyl- and *N*-carbamoyl-racemase
333 activities [8,29,30,34], our results show that DrcNSAAR racemizes *N*-formyl-
334 methionine faster than the *N*-acetyl- and *N*-carbamoyl-derivatives, as observed with
335 GstNSAAR and GkaNSAAR. Whereas GkaNSAAR has been the first NSAAR enzyme
336 successfully used in the DKR of *N*-formyl-amino acids [32,33], kinetic studies with *N*-
337 formyl-amino acids had not been conducted previously [9]. Thus, kinetic parameters
338 were obtained from hyperbolic saturation curves by least-squares fit of the data to the
339 Michaelis-Menten equation (Figure 5A). Reactions were carried out with different *N*-
340 formyl-amino acids at varying concentrations (1-50 mM) at 45 °C and pH 8.0. The best
341 substrate among those tested was *N*-formyl-homophenylalanine, with both the lowest
342 K_m and highest k_{cat} values (Table 4). Taking into account the errors associated with the
343 measurements, the first conclusion is that GstNSAAR presents a slightly higher
344 catalytic efficiency toward the D-enantiomer of the substrates in most cases, similarly to
345 the results observed previously with GkaNSAAR using *N*-acetyl-amino acids as
346 substrates [9]. The k_{cat}/K_m values of GstNSAAR towards *N*-formyl-amino acids was in
347 the 10^3 - 10^4 $M^{-1}\cdot s^{-1}$ range (Table 4), whereas GkaNSAAR catalytic efficiency was in the
348 10 - 10^3 $M^{-1}\cdot s^{-1}$ range with *N*-acetyl-amino acids [9]. Unexpectedly, the catalytic

349 efficiency of GstNSAAR towards *N*-formyl-amino acids was in the same range than the
350 obtained for the natural substrates of *G. kaustophilus* HTA426 NSAAR (*N*-succinyl-
351 amino acids; 10^3 - 10^4 M⁻¹·s⁻¹) [16]. In fact, and whereas slightly lower, kinetic K_m and
352 k_{cat} values of GstNSAAR towards *N*-formyl-L-methionine (9.0 ± 0.8 mM, 52.9 ± 1.4 s⁻¹)
353 were very similar to those of *G. kaustophilus* HTA426 NSAAR with *N*-succinyl-L-
354 methionine (3.6 ± 0.4 mM, 53.0 ± 1.0 s⁻¹) [16]. In *G. kaustophilus* HTA426, NSAAR
355 appears in an operon together with highly enantioselective succinyl-CoA:D-amino acid
356 *N*-succinyltransferase and *N*-succinyl-L-amino acid hydrolase enzymes, conforming a
357 metabolic pathway for irreversible conversion of D-amino acids to their L-enantiomers
358 [16,17]. Despite the suggested moonlight character of NSAAR [16], based on the
359 previous results on the isolated enzymes in the *G. kaustophilus* HTA426 “succinyl-
360 transferase/racemase/hydrolase” operon (where less than 0.1% of hydrolase activity was
361 detected towards *N*-formyl-amino acids), the similar efficiency of GstNSAAR towards
362 *N*-formyl- and *N*-succinyl-amino acids do not seem to support the former as an
363 alternative natural substrate for this route.

364

365 When analyzing the *N*-formyl-amino acid racemization of GstNSAAR, GkaNSAAR
366 and DrcNSAAR, the catalytic efficiency values using *N*-formyl-D-norleucine were
367 1.9 ± 0.3 , 1.7 ± 0.3 and 0.2 ± 0.0 s⁻¹·mM⁻¹, respectively. Thus, *Geobacillus* enzymes
368 presented an efficiency one order of magnitude higher than that of the *Deinococcus*
369 enzyme, in accordance with the trend of the specific activities for the other *N*-
370 substituted-amino acids (Table 2). Our results show that from a biotechnological point
371 of view, even though DraNSAAR has been successfully applied in different DKR
372 processes [29,30,34], GstNSAAR and GkaNSAAR enzymes might be better candidates

373 for putative industrial applications based on their higher activities with the substrates
374 assayed (Table 2).

375

376 *Effect of residues K166, D191, E216, D241 and K265 on the activity of GstNSAAR*

377 Previous mutagenesis studies carried out with *Amycolatopsis* sp T-1-160 NSAAR
378 already concluded that NSAAR enzymes use a two-base mechanism for racemization,
379 more specifically two lysine residues [13]. The crystallographic structure of this enzyme
380 (PDB ID. 1SJA) showed three additional residues involved in substrate binding [14].
381 The five counterpart residues of GstNSAAR are K166, D191, E216, D241 and K265.
382 We decided to mutate these residues to alanine in order to evaluate their implication in
383 the activity and binding of GstNSAAR. Purity of the mutants was over 95% (data not
384 shown). Far-UV CD spectra were collected to evaluate the native-like folding of the Co-
385 amended mutants. No significant differences were found in the far-UV CD spectra of
386 the five alanine mutants, and we can therefore conclude that their secondary structure is
387 basically the same as that of wild-type NSAAR (data not shown). Thermal melts were
388 irreversible, as for the wild-type enzyme, but we determined the $T_{m(app)}$ values for all the
389 mutants (Table 3). Since the temperature melts were irreversible, these values should be
390 only considered as a qualitative measure of the similar stability of the WT and mutated
391 species. Except for the thermal midpoint obtained for K265A mutant, which was higher
392 than the rest, the melting curves, together with the steady-state far-UV data, suggest that
393 the alanine scanning mutations did not alter significantly the native-like structure of the
394 enzyme.

395

396 All the mutants showed negligible activity using up to 50 μ M of enzyme (Table 3),
397 confirming their key role in substrate racemization. Binding experiments with the

398 alanine mutants using *N*-formyl-D- and *N*-formyl-L-methionine (Figure 5B) yielded
399 affinity constants in the range of 10^3 - 10^4 M⁻¹ (Table 5), showing a slightly higher
400 affinity for the D-enantiomer in all cases, and confirming these residues as not
401 indispensable for *N*-formyl-amino acid binding despite its key role in the enzyme
402 activity (Table 3). These results follow the same trend as the catalytic efficiency of the
403 enzyme toward the different enantiomer pairs (Table 4), which also present a slight
404 preference for the D-enantiomer. This slight preference agrees with the expected
405 enantioselectivity of an NSAAR participating in the irreversible conversion of D-amino
406 acids to their L-enantiomers using the above mentioned “succinyl-
407 transferase/racemase/hydrolase” operon [16]. Although the genome of *G.*
408 *stearothermophilus* CECT49 is not available, **the one from** *G. stearothermophilus* str.
409 53 (GenBank Acc. No. JPYV01000018) also contains the counterpart operon,
410 suggesting that this gene organization also might be present in *G. stearothermophilus*
411 CECT49.

412

413 Since the $T_{m(\text{app})}$ values for the three metal-binding mutants (D191A, E216A and
414 D241A) were very similar to that found for the wild-type NSAAR (Table 3), we could
415 argue that the three mutants are still able to bind the cation, since the presence of Co²⁺
416 produced a 10 °C increase in the thermal **midpoint** (see above). Whereas we cannot
417 compare the affinity constants with those of the wild-type (they cannot be obtained as
418 both isomers would be in solution), the affinity of the three mutants for both ligands
419 decreased in the order D191A > D241A > E216A. By similarity of GstNSAAR and
420 DraNSAAR (PDB ID 1XPY, [8]) the observed decrease in affinity might be a reflect of
421 a lower polarization of the Co²⁺ cofactor by the absence of one of the carboxylate group
422 of the lateral chains of the three amino acids, altering the interaction of the cation with
423 the carboxylate group of the substrate. However, this cation-carboxylate interaction is

424 not totally indispensable for substrate binding, since we also confirmed that the three
425 mutants are able to bind both enantiomers of the substrate, although with slightly lower
426 affinity (data not shown). The absence of activity of the D191A, E216A and D241A
427 mutants (Table 3) also suggest that the proposed role of stabilization of the enediolate
428 anion intermediate of the reaction by the cofactor, is indispensable for the proposed
429 two-base 1,1-proton transfer mechanism [8, 13]: mutation of any of the three-binding
430 residues inactivates the enzyme, even when the cation is bound to the enzyme,
431 hampering the racemization of the substrate.

432

433 The results with the K166A and K265A mutants are similar to those obtained
434 previously for *Amycolatopsis* NSAAR [13]: mutation of these residues also inactivated
435 GstNSAAR. These results are in accordance with the proposed two-base mechanism of
436 the enolase superfamily [8,13]. It is worth noting the apparent enhancement of K265A
437 $T_{m(\text{app})}$ (Table 3) and the apparent higher affinity of K166A towards *N*-formyl-D-
438 methionine (Table 5). In the absence of additional results, we could only speculate on
439 both interesting features. The homolog DraNSAAR X-Ray structure (PDB ID 1XPY,
440 [8]) shows that the counterpart lysine residues (K168_{Dra} and K269_{Dra}) are situated 3.8 Å
441 away from the cation. Since our results show that: *i*) the presence of the cation increases
442 the GstNSAAR $T_{m(\text{app})}$ and *ii*) mutation in the metal-binding residues and the presence
443 of the cation alter the affinity of GstNSAAR by the substrates (Table 5), we could argue
444 that K166A and K265A mutations might produce alterations in the environment of the
445 Co^{2+} cation, producing two different effects. In one hand, K265A mutation might result
446 in a tighter binding of the cofactor, resulting in an even higher stabilization of the
447 tertiary structure of GstNSAAR, thus increasing its $T_{m(\text{app})}$. On the other hand, since the
448 counterpart of K166 and D191 in the DraNSAAR structure (K168_{Dra} and D195_{Dra}; PDB

449 ID 1XPY, [8]) are positioned 2.8 Å away, we could argue that if K166-D191 interaction
450 is lost due to the mutation, changes in the polarizability of the cation might occur, thus
451 altering the affinity by the different ligands (Table 5).

452

453 **Conclusion**

454

455 Several studies carried out by Glasner's group have previously highlighted two specific
456 difficulties to find new NSAAR enzymes. Firstly, the high degree of similarity between
457 the OSBS family [40] complicates the discovery of real NSAAR enzymes, since even
458 members of the so-called *Firmicutes* NSAR/OSBS subfamily are not active towards *N*-
459 succinyl-amino acids [10]. Secondly, several works have proven the difficulties to find
460 the determinant allowing the evolution of OSBS family towards NSAAR activity
461 [40,46,47]. The recent published studies on the role of the 20s loop of *Amycolatopsis* sp
462 T-1-160 NSAAR [47] has shed some light on the importance of the conservation of not
463 only the five residues mutated in this work, but other residues previously observed in
464 the substrate-bound crystallographic structure of DraNSAAR (Figure 2) [8]. In our
465 opinion, an alternative clue to find new biotechnologically relevant NSAAR
466 enzymes/sequences, different to the only three for which a sequence-activity
467 relationship has been proven (*Geobacillus*, *Deinococcus*, *Amycolaptosis*), might lie on
468 the localization of similar *N*-succinyl-“transferase/racemase/hydrolase” operons similar
469 to that reported previously [16].

470

471

472

473

474 **References**

475 1.- May, O., Verseck, S., Bommarius, A. and Drauz, K. (2002) Development of
476 dynamic kinetic resolution processes for biocatalytic production of natural and
477 nonnatural L-amino acids. *Org. Process Res. Dev.* 6, 452-457.

478

479 2.- Tokuyama, S., Hatano, K. and Takahashi, T. (1994) Discovery of a novel enzyme,
480 N-acylamino acid racemase in an actinomycete: screening, isolation and identification.
481 *Biosci. Biotech. Biochem.* 58, 24-27.

482

483 3.- Tokuyama, S., Miya, H., Hatano, K. and Takahashi, T. (1994) Purification and
484 properties of a novel enzyme, N-acylamino acid racemase, from *Streptomyces atratus*
485 Y-53. *Appl. Microbiol. Biotechnol.* 40, 835-840.

486

487 4.- Tokuyama, S. and Hatano, K. (1995) Purification and properties of thermostable N-
488 acylamino acid racemase from *Amycolatopsis* sp. TS-1-60. *Appl. Microbiol.*
489 *Biotechnol.* 42, 853-859.

490

491 5.- Tokuyama, S. and Hatano, K. (1995) Cloning, DNA sequencing and heterologous
492 expression of the gene for thermostable N-acylamino acid racemase from *Amycolatopsis*
493 sp. TS-1-60 in *Escherichia coli*. *Appl. Microbiol. Biotechnol.* 42, 884-889.

494

495 6.- Verseck, S., Bommarius, A. and Kula, M.R. (2001) Screening, overexpression and
496 characterization of an N-acylamino acid racemase from *Amycolatopsis orientalis* subsp.
497 *lurida*. *Appl. Microbiol. Biotechnol.* 55, 354-361.

498

499 7.- Su, S.-C. and Lee, C.-Y. (2002) Cloning of the N-acylamino acid racemase gene
500 from *Amycolatopsis azurea* and biochemical characterization of the gene product.
501 *Enzyme Microb. Technol.* 30, 647-655.
502

503 8.- Wang, W.C., Chiu, W.C., Hsu, S.K., Wu, C.L., Chen, C.Y., Liu, J.S. and Hsu, W.H.
504 (2004) Structural basis for catalytic racemization and substrate specificity of an N-
505 acylamino acid racemase homologue from *Deinococcus radiodurans*. *J. Mol. Biol.* 342,
506 155-169.
507

508 9.- Pozo-Dengra, J., Martinez-Gomez, A.I., Martinez-Rodriguez, S., Clemente-Jimenez,
509 J.M., Rodriguez-Vico, F. and Las Heras-Vazquez, F.J. (2009) Racemization study on
510 different N-acetylamino acids by a recombinant *N*-succinylamino acid racemase from
511 *Geobacillus kaustophilus* CECT4264. *Process Biochem.* 44, 835-841.
512

513 10.- Palmer, D.R., Garrett, J.B., Sharma, V., Meganathan, R., Babbitt, P.C. and Gerlt,
514 J.A. (1999) Unexpected divergence of enzyme function and sequence: "N-acylamino
515 acid racemase" is o-succinylbenzoate synthase. *Biochemistry.* 38, 4252-4258.
516

517 11.- Thompson, T.B., Garrett, J.B., Taylor, E.A., Meganathan, R., Gerlt, J.A. and
518 Rayment, I. (2000) Evolution of enzymatic activity in the enolase superfamily: structure
519 of o-succinylbenzoate synthase from *Escherichia coli* in complex with Mg²⁺ and o-
520 succinylbenzoate. *Biochemistry.* 39, 10662-10676.
521

522 12.- Schmidt, D.M., Hubbard, B.K. and Gerlt, J.A. (2001) Evolution of enzymatic
523 activities in the enolase superfamily: functional assignment of unknown proteins in

524 *Bacillus subtilis* and *Escherichia coli* as L-Ala-D/L-Glu epimerases. *Biochemistry*.
525 4051, 15707-15715.
526
527
528 13.- Taylor Ringia, E.A., Garrett, J.B., Thoden, J.B., Holden, H.M., Rayment, I. and
529 Gerlt, J.A. (2004) Evolution of enzymatic activity in the enolase superfamily: functional
530 studies of the promiscuous o-succinylbenzoate synthase from *Amycolatopsis*.
531 *Biochemistry*. 43, 224-229.
532
533 14.- Thoden, J.B., Taylor Ringia, E.A., Garrett, J.B., Gerlt, J.A., Holden, H.M., and
534 Rayment, I. (2004) Evolution of enzymatic activity in the enolase superfamily:
535 structural studies of the promiscuous o-succinylbenzoate synthase from *Amycolatopsis*.
536 *Biochemistry*. 43, 5716-5727.
537
538 15.- Glasner, M.E., Fayazmanesh, N., Chiang, R.A., Sakai, A., Jacobson, M.P., Gerlt,
539 J.A. and Babbitt, P.C. (2006) Evolution of structure and function in the o-
540 succinylbenzoate synthase/N-acylamino acid racemase family of the enolase
541 superfamily. *J. Mol. Biol.* 360, 228-250.
542
543 16.- Sakai, A., Xiang, D.F., Xu, C., Song, L., Yew, W.S., Raushel, F.M. and Gerlt, J.A.
544 (2006) Evolution of enzymatic activities in the enolase superfamily: *N*-succinylamino
545 acid racemase and a new pathway for the irreversible conversion of D- to L-amino
546 acids. *Biochemistry*. 45, 4455-4462.
547

548 17.- Song, L., Kalyanaraman, C., Fedorov, A.A., Fedorov, E.V., Glasner, M.E., Brown,
549 S., Imker, H.J., Babbitt, P.C., Almo, S.C., Jacobson, M.P. and Gerlt, J.A. (2007)
550 Prediction and assignment of function for a divergent N-succinyl amino acid racemase.
551 Nat. Chem. Biol. 3, 486–491.
552

553 18.- Bommarius A, Drauz K, Kula M-R, Verseck S. (2001) N-Acetylamino acid
554 racemase. EP 1074628 A1.
555

556 19.- Bommarius, A., Drauz, K., Verseck, S. and Kula, M.-R. (2004) Acetyl amino acid
557 racemase from *Amycolatopsis orientalis* for racemizing carbamoyl amino acids. US
558 Patent 6767725 B2.
559

560 20.- Bommarius, A., Drauz, K. and Verseck, S. (2008) Racemization and deprotection
561 of special N-protected amino acids in the acylase/racemase system for the total
562 conversion of special N-protected racemic amino acids into optically pure amino acids.
563 US Patent 7378269 B2.
564

565 21.- Verseck, S., Kula, M.-R, Bommarius, A. and Drauz, K. (2002) For producing
566 enantiomer-enriched amino acids, and derivatives US Patent 6372459 B1.
567

568 22.- Takahashi, T. and Hatano, K. (1989) Acylamino acid racemase, Production and use
569 thereof. EP 0304021 A2.
570

571 23.- Takahashi, T. and Hatano, K. (1991) Acylamino acid racemase, production and use
572 thereof. US Patent 4981799 A.

573

574 24.- Tokuyama, M., Hatano, K., Nakahama, K. and Takahashi, T. (1992) DNA
575 encoding acylamino acid racemase and its use. EP 0474965 A2.

576

577 25.- Srivibool, R., Kurakami, K., Sukchotiratana, M. and Tokuyama, S. (2004) Coastal
578 soil actinomycetes: thermotolerant strains producing N-acylamino acid racemase.
579 Science Asia 30, 123-126.

580

581 26.- Tokuyama, S. and Hatano, K. (1996) Overexpression of the gene for N-acylamino
582 acid racemase from *Amycolatopsis* sp. TS-1-60 in *Escherichia coli* and continuous
583 production of optically active methionine by a bioreactor. Appl. Microbiol. Biotechnol.
584 44, 774-777.

585

586 27.- Chiu, W.C., You, J.Y., Liu, J.S., Hsu, S.K., Hsu, W.H., Shih, C.H., Hwang, J.K.
587 and Wang, W.C. (2006) Structure-stability-activity relationship in covalently cross-
588 linked N-carbamoyl-D-amino acid amidohydrolase and N-acylamino acid racemase. J.
589 Mol. Biol. 359, 741-753.

590

591 28.- Hsu, S.K., Lo, H.H., Kao, C.H., Lee, D.S. and Hsu, W.H. (2006) Enantioselective
592 synthesis of L-homophenylalanine by whole cells of recombinant *Escherichia coli*
593 expressing L-aminoacylase and N-acylamino acid racemase genes from *Deinococcus*
594 *radiodurans* BCRC12827. Biotechnol. Prog. 22, 1578-1584.

595

596 29.- Hsu, S., Lo, H., Lin, W., Chen, I., Kao, C. and Hsu, W. (2007) Stereoselective
597 synthesis of L-homophenylalanine using the carbamoylase method with in situ
598 racemization via N-acylamino acid racemase. *Process Biochem.* 42, 856–862.
599

600 30.- Yen, M.-C., Hsu, W.-H. and Lin S.-C. (2010) Synthesis of L-homophenylalanine
601 with immobilized enzymes. *Process Biochem.* 45, 667-674.
602

603 31.- Pozo-Dengra, J., Martínez-Rodríguez, S., Contreras, L.M., Prieto, J., Andújar-
604 Sánchez, M., Clemente-Jiménez, J.M., Las Heras-Vázquez, F.J., Rodríguez-Vico, F.
605 and Neira, J.L. (2009) Structure and conformational stability of a tetrameric
606 thermostable N-succinylamino acid racemase. *Biopolymers* 91, 757-772.
607

608 32.- Soriano-Maldonado, P., Rodríguez-Alonso, M.J., Hernández-Cervantes,
609 C., Rodríguez-García, I., Clemente-Jiménez, J.M., Rodríguez-Vico, F., Martínez-
610 Rodríguez, S. and Las Heras-Vázquez, F.J. (2014) Amidohydrolase Process: Expanding
611 the use of L-N-carbamoylase/N-succinyl-amino acid racemase tandem for the
612 production of different optically pure L-amino acids. *Process Biochem.* 49, 1281-1287.
613

614 33.- Soriano-Maldonado, P., Las Heras-Vazquez, F.J., Clemente-Jimenez, J.M.,
615 Rodriguez-Vico, F., Martínez-Rodríguez, S. (2014) Enzymatic dynamic kinetic
616 resolution of racemic N-formyl- and N-carbamoyl-amino acids using immobilized L-N-
617 carbamoylase and N-succinyl-amino acid racemase. *Appl. Microbiol. Biotechnol.* doi
618 10.1007/s00253-014-5880-7.
619

620 34.- Hayashida, M., Kim, S.H., Takeda, K., Hisano, T. and Miki, K. (2008) Crystal
621 structure of N-acylamino acid racemase from *Thermus thermophilus* HB8. *Proteins* 71,
622 519-523.
623

624 35.- Baxter, S., Royer, S., Grogan, G., Brown, F., Holt-Tiffin, K.E., Taylor, I.N.,
625 Fotheringham, I.G. and Campopiano, D.J. (2012) An improved racemase/acylase
626 biotransformation for the preparation of enantiomerically pure amino acids. *J. Am.*
627 *Chem. Soc.* 134, 19310-19313.
628

629 36.- Martínez-Rodríguez, S., Martínez-Gómez, A.I., Rodríguez-Vico, F., Clemente-
630 Jiménez, J.M. and Las Heras-Vázquez, F.J. (2010) N-Carbamoyl-D- and L-amino acid
631 amidohydrolases: characteristics and applications in biotechnological processes. *Appl.*
632 *Microbiol. Biotechnol.* 85, 441-458.
633

634 37.- Stumpp T, Wilms B, Altenbuchner J. (2000) Ein neues, L-rhamnoseinduzierbares
635 expressionssystem für *Escherichia coli*. *Biospektrum* 6, 33-36.
636

637 38.- Larkin, M.A., Blackshields, G., Brown, N.P., Chenna, R., McGettigan, P.A.,
638 McWilliam, H., Valentin, F., Wallace, I.M., Wilm, A., Lopez, R., Thompson, J.D.,
639 Gibson, T.J. and Higgins, D.G. (2007) Clustal W and Clustal X version 2.0.
640 *Bioinformatics* 23, 2947-2948.
641

642 39.- Gill, S.C. and von Hippel, P.H. (1989) Calculation of protein extinction coefficients
643 from amino acid sequence data, *Anal. Biochem.* 182, 319-326.
644

645 40.- Zhu, W.W., Wang, C., Jipp, J., Ferguson, L., Lucas, S.N., Hicks, M.A., Glasner,
646 M.E. (2012) Residues required for activity in *Escherichia coli* o-succinylbenzoate
647 synthase (OSBS) are not conserved in all OSBS enzymes. *Biochemistry*. 51, 6171-6181.
648

649 41.- Babbitt, P.C., Hasson, M.S., Wedekind, J.E., Palmer, D.R., Barrett, W.C., Reed,
650 G.H., Rayment, I., Ringe, D., Kenyon, G.L. and Gerlt JA. (1996) The enolase
651 superfamily: a general strategy for enzyme-catalyzed abstraction of the alpha-protons of
652 carboxylic acids. *Biochemistry*. 35, 16489-16501.
653

654 42.- Galisteo, M.L., Mateo, P.L. and Sánchez-Ruiz, J.M. (1991) Kinetic study on the
655 irreversible thermal denaturation of yeast phosphoglycerate kinase, *Biochemistry*. 30,
656 2061-2066.
657

658 43.- Martínez-Rodríguez, S., Encinar, J.A., Hurtado-Gómez, E., Prieto, J., Clemente-
659 Jiménez, J.M., Las Heras-Vázquez, F.J., Rodríguez-Vico, F. and Neira, J.L. (2009)
660 Metal-triggered changes in the stability and secondary structure of a tetrameric
661 dihydropyrimidinase: a biophysical characterization. *Biophys. Chem*. 139, 42-52.
662

663 44.- Eissenthal, R., Peterson, M. E., Daniel, R. M. and Danson, M. J. (2006) The thermal
664 behaviour of enzyme activity: implications for biotechnology. *Trends Biotechnol*. 24,
665 289-292.
666

667 45.- Daniel, R.M., Peterson, M.E., Danson, M.J., Price, N.C., Kelly, S.M., Monk, C.R.,
668 Weinberg, C.S., Oudshoorn, M.L. and Lee, C.K. (2009) The molecular basis of the
669 effect of temperature on enzyme activity. *Biochem. J*. 425, 3533-60.

670

671 46.- Odokonyero, D., Ragumani, S., Lopez, M.S., Bonanno, J.B., Ozerova, N.D.,
672 Woodard, D.R., Machala, B.W., Swaminathan, S., Burley, S.K., Almo, S.C., Glasner,
673 M.E. (2013) Divergent evolution of ligand binding in the o-succinylbenzoate synthase
674 family. *Biochemistry* 52, 7512-7521.

675

676 47.- McMillan, A.W., Lopez, M.S., Zhu, M., Morse, B.C., Yeo, I.C., Amos, J., Hull, K.,
677 Romo, D., Glasner, M.E. (2014) Role of an active site loop in the promiscuous activities
678 of *Amycolatopsis* sp. T-1-60 NSAR/OSBS. *Biochemistry* 53, 4434-4444.

679

680

681

682

683

684

685

686

687

688

689

690

691

692

693

694

695

696 **Table 1.** Relative activity of GstNSAAR in the presence of different mono- and
697 divalent cations, using the cobalt-amended GstNSAAR as reference. The effect of the
698 different cations was assayed using the apo-form of GstNSAAR. Values are the mean of
699 three experiments, and the error indicates the standard deviation of the mean.

700

701

702

703

704

705

	Sample	Relative activity (%)
706	apo-GstNSAAR	0.0±0.0
	Co ²⁺	100.0±1.1
707	Ni ²⁺	55.8±7.6
	K ⁺	40.22±8.4
708	Na ⁺	42.8±10.4
	Li ⁺	45.8±5.4
	Cs ⁺	47.8±12.9
709	Rb ⁺	40.8±8.5
	Mg ²⁺	28.1±2.9
710	Ca ²⁺	14.3±0.7
	Zn ²⁺	14.4±6.5
711	Fe ²⁺	15.5±0.6
	Hg ²⁺	3.7±4.0
712	Pb ²⁺	8.3±0.9

713

714

715

716

717

718

719 **Table 2.** Specific activities ($\mu\text{mol}\cdot\text{min}^{-1}\cdot\text{mg}$ of enzyme⁻¹) of the different enzymes used
720 in this work toward different *N*-substituted amino acids. Reaction conditions were the
721 same in all cases for values to be comparable among them (15 mM substrate in 100 mM
722 Borate-HCl 1.6 mM CoCl₂ pH 8.0, at 45 °C)

723

724

725

	GKaNSAAR	GstNSAAR	DrcNSAAR
<i>N</i> -Succinyl-D-phenylalanine	3.3±1.0	3.3±0.2	2.4±0.1
<i>N</i> -Succinyl-L-phenylalanine	7.9±1.0	9.0±0.2	4.5±0.2
<i>N</i> -Formyl-D-methionine	4.7±0.3	4.9±0.5	2.6±0.4
<i>N</i> -Acetyl-D-methionine	3.6±0.0	3.7±0.0	1.6±0.0
<i>N</i> -Carbamoyl-D-methionine	0.7±0.1	0.7±0.1	0.3±0.1
<i>N</i> -Formyl-D-norleucine	1.7±0.3	1.9±0.3	0.2±0.0
<i>N</i> -Carbamoyl-D-norleucine	0.3±0.0	0.3±0.0	0.1±0.0

729

730

731

732

733

734

735

736

737

738

739

740

741

742

743 **Table 3.** Thermal denaturation midpoints obtained for GstNSAAR and mutants in the
744 presence of CoCl₂, and relative activities of the mutants using *N*-formyl-D- and *N*-
745 formyl-L-methionine, compared to the wild-type enzyme.

746

Enzyme	Thermal denat. midpoint (° C)	Relative activity (%) <i>N</i>-formyl-D-MET	Relative activity (%) <i>N</i>-formyl-L-MET
GstNSAAR	77.0±0.1	100.00	100.00
K166A	78.5±0.1	0.02	0.01
D191A	76.5±0.1	0.00	0.02
E216A	78.7±0.1	0.01	0.01
D241A	76.9±0.1	0.01	0.02
K265A	83.4±0.6	0.01	0.04

747

748

749

750

751

752

753

754

755

756

757

758

759

760

761

762

763 **Table 4. Kinetic analyses of wild-type GstNSAAR.** Kinetic parameters were obtained
 764 from hyperbolic saturation curves by least-squares fit of the data to the Michaelis-
 765 Menten equation. Reactions were carried out with the different *N*-formyl-amino acids at
 766 different concentrations (1-50 mM) at 45 °C and pH 8.0.

767

Substrate	K_m (mM)	<i>k</i>_{cat} (s⁻¹)	<i>k</i>_{cat}/K_m (s⁻¹·mM⁻¹)
<i>N</i> -Formyl-D-methionine	12.6±2.7	74.6±5.1	5.9±1.7
<i>N</i> -Formyl-L-methionine	9.0±0.8	52.9±1.4	5.9±0.7
<i>N</i> -Formyl-D-norleucine	11.1±4.1	12.3±1.4	1.1±0.5
<i>N</i> -Formyl-L-norleucine	12.5±1.7	8.0±0.4	0.6±0.1
<i>N</i> -Formyl-D-aminobutyric acid	19.6±3.7	15.2±0.7	0.8±0.2
<i>N</i> -Formyl-L-aminobutyric acid	17.9±2.5	11.6±0.7	0.7±0.1
<i>N</i> -Formyl-D-norvaline	9.2±1.8	11.2±0.7	1.3±0.3
<i>N</i> -Formyl-L-norvaline	24.5±5.7	19.6±1.4	0.8±0.2
<i>N</i> -Formyl-D-homophenylalanine	3.0±0.7	88.4±4.3	29.5±8.3
<i>N</i> -Formyl-L-homophenylalanine	5.7±0.5	85.5±0.7	15.0±1.4

768

769

770

771

772

773

774

775

776

777

778

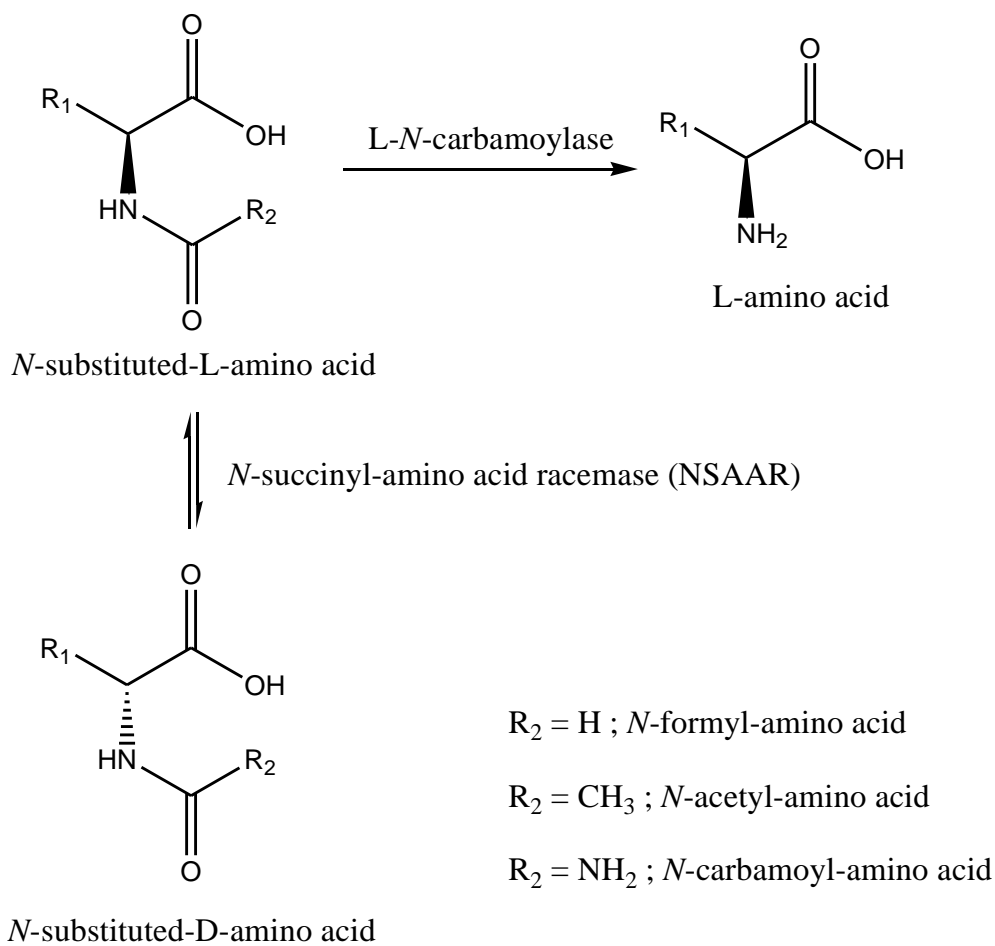
779 **Table 5.** Binding constants obtained for *N*-formyl-D- and *N*-formyl-L-methionine
780 GstNSAAR mutants. Titration was performed at 25 °C in 100 mM Borate-HCl 1.6 mM
781 CoCl₂ pH 8.0. Enzyme concentrations were in the range 0.8-1.0 μM and were titrated
782 by addition of different ligand volume of solution at a concentration of 50 mM of *N*-
783 formyl-D- or *N*-formyl-L-methionine.
784

GstNSAAR mutant	Ligand	K (M ⁻¹)	Ratio D/L
K265A	<i>N</i> -Formyl-L-methionine	1017±22	1.7
	<i>N</i> -Formyl-D-methionine	1689±27	
D191A	<i>N</i> -Formyl-L-methionine	1871±18	1.2
	<i>N</i> -Formyl-D-methionine	2195±19	
D241A	<i>N</i> -Formyl-L-methionine	1444±12	1.4
	<i>N</i> -Formyl-D-methionine	2024±24	
E216A	<i>N</i> -Formyl-L-methionine	1113±39	1.2
	<i>N</i> -Formyl-D-methionine	1343±21	
K166A	<i>N</i> -Formyl-L-methionine	1792±33	2.9
	<i>N</i> -Formyl-D-methionine	5269±38	

796
797
798
799
800
801
802
803
804
805
806

807 **Figure 1.** Reaction scheme for optically pure L-amino acid production from racemic
 808 mixtures of *N*-substituted-amino acids using the “Amidohydrolase process”. $R_1 =$
 809 lateral chain of the corresponding amino acid. $R_2 = N$ -substituent. In the original
 810 “Acylase Process”, $R_2 = \text{CH}_3$.

811



812

813

814

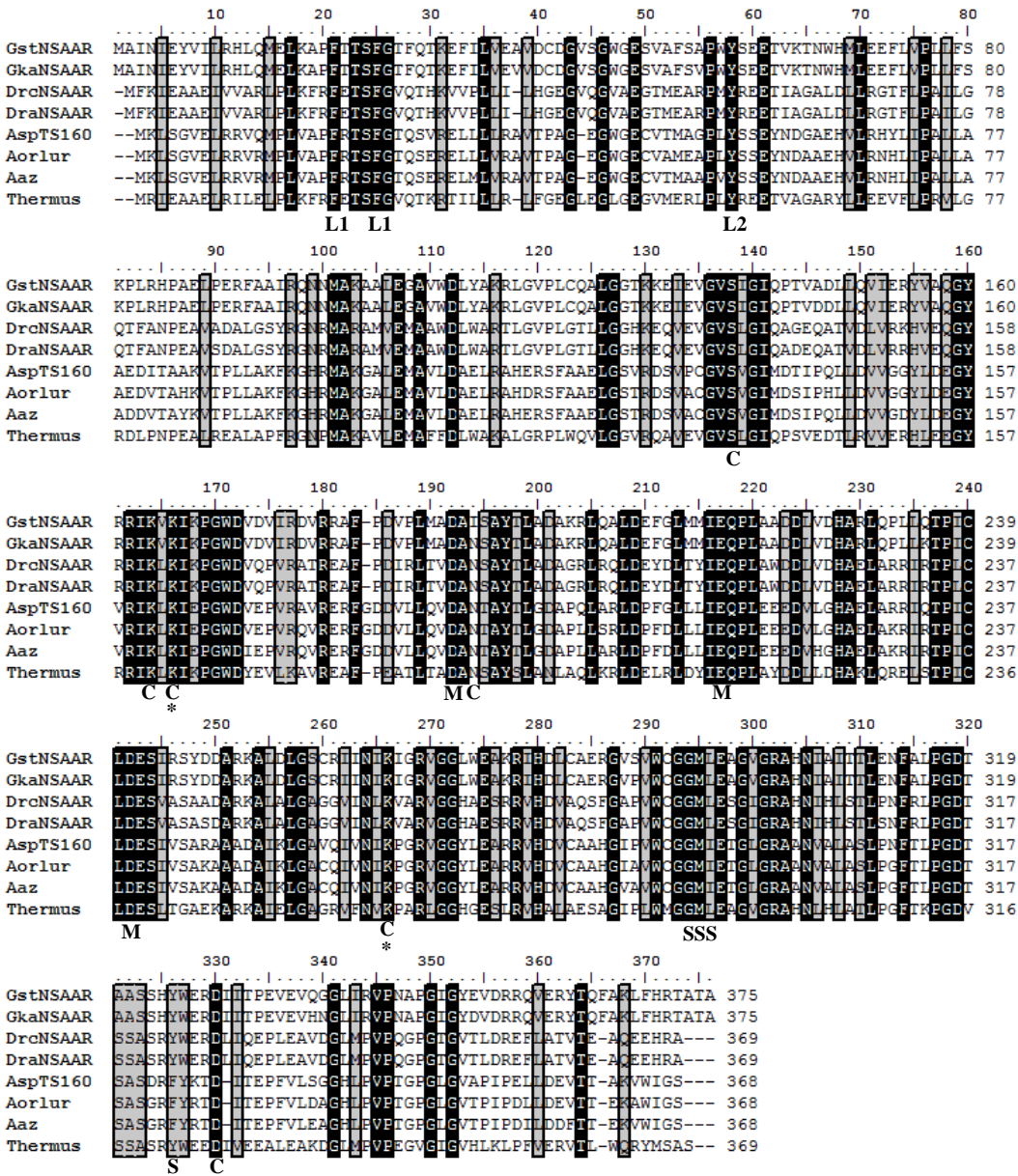
815

816

817

818

819 **Figure 2.** Sequence alignment of the different NSAAR enzymes reported in the
820 literature. GstNSAAR, NSAAR from *Geobacillus stearothermophilus* CECT49 (this
821 work); GkaNSAAR, NSAAR from *Geobacillus kaustophilus* CECT4264, GenBank
822 accession no. ABZ81711 [31]; DrcNSAAR, NSAAR from *Deinococcus radiodurans*
823 CECT833 (this work); DraNSAAR, NSAAR from *Deinococcus radiodurans*, GenBank
824 accession no. 1R0M [8]; AspTS160, NSAAR from *Amycolatopsis* sp. TS-1-60,
825 GenBank accession no. BAA06400 [4,5]; Aorlur, NSAAR from *Amycolatopsis*
826 *orientalis* subsp. *lurida*, GenBank accession no. CAC00653 [6]; Aaz, NSAAR from
827 *Amycolatopsis azurea*, GenBank accession no. AF335269_1 [7]; Thermus, putative
828 NSAAR from *Thermus thermophilus*, accession No BAD70697.1 [34]. The residues
829 predicted to most likely configure the catalytic pocket of DraNSAAR are highly
830 conserved among the different NSAAR above described, and are shown under the
831 alignment with letters following the original nomenclature [8] (C: carboxyl group-
832 binding site; M: metal-binding site; L1 and L2: L region; S: side-chain-binding region).
833



835

836

837

838

839

840

841

842

843

844 **Figure 3.** Size exclusion chromatography elution profile of GstNSAAR using a
845 Superdex 200 10/300 column. The inset represents the SDS-PAGE of the different
846 purified recombinant NSAAR enzymes. Lane 1, low molecular weight marker; lanes 2,
847 3, and 4, purified GstNSAAR, GkaNSAAR, and DrcNSAAR, respectively.

848

849

850

851

852

853

854

855

856

857

858

859

860

861

862

863

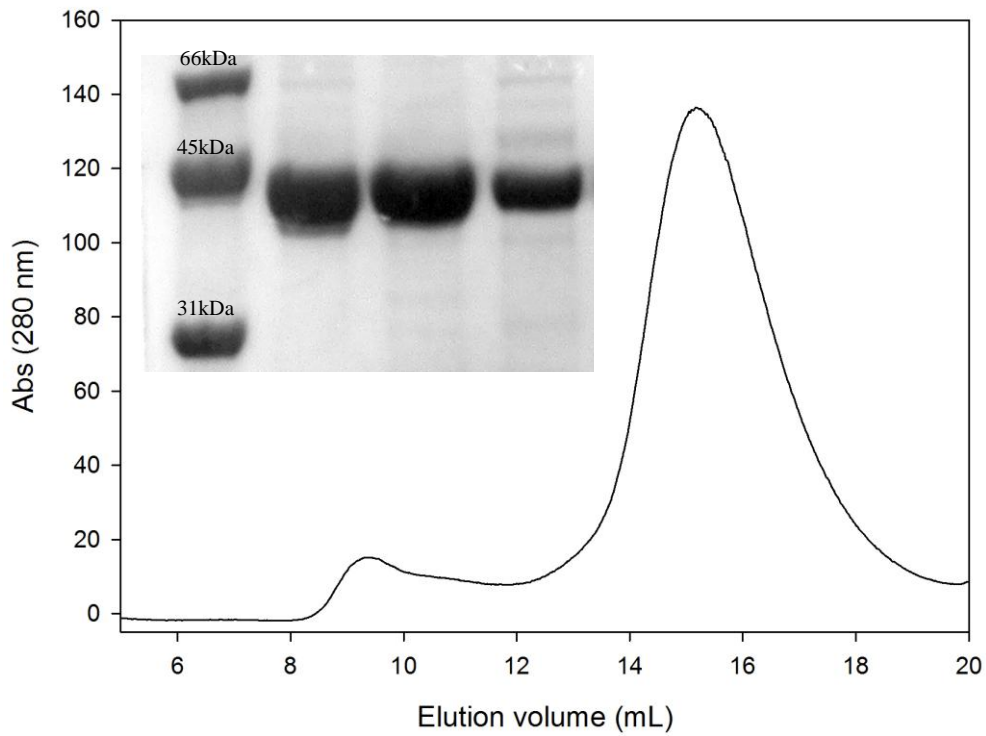
864

865

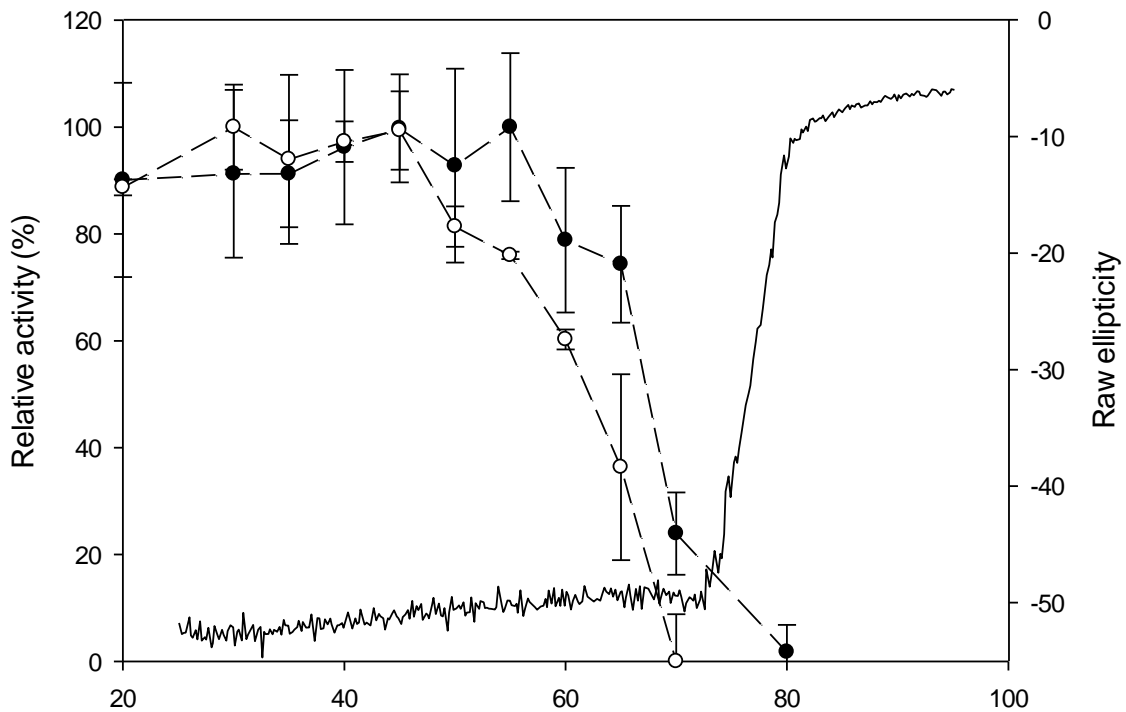
866

867

868



869 **Figure 4.** CD-Thermal denaturation of cobalt amended GstNSAAR followed by the
870 changes in ellipticity at 222 nm (continuous line, right axis). The plot also shows the
871 remaining relative activity of GstNSAAR after 60-min preincubation at the
872 corresponding temperature, both in the presence (●) and absence (○) of Co^{2+} (left axis).
873 The results showing the remaining activity of GstNSAAR are the mean of three
874 experiments, and the error bars indicate the standard deviation of the mean.
875



876

877

878

879

880

881

882

883

884 **Figure 5.** A) Kinetics of GstNSAAR using *N*-formyl-L-homophenylalanine as substrate
885 (45 °C and pH 8.0). The results are the mean of three experiments, and the error bars
886 indicate the standard deviation of the mean. B) Fluorescence titration of *N*-formyl-D-
887 methionine binding to E216A and K166A GstNSAAR mutants. Titrations were
888 performed in 100 mM Borate-HCl buffer pH 8.0 and 25 °C, with enzyme concentrations
889 in the range 0.81-0.95 μM. Stock ligand concentrations were 50 mM.

890

891

892

893

894

895

896

897

898

899

900

901

902

903

904

905

906

